

## Alterations in the Determinants of Diastolic Suction During Pacing Tachycardia

Stephen P. Bell, Lori Nyland, Marc D. Tischler, Mark McNabb, Henk Granzier, Martin M. LeWinter

**Abstract**—In cardiomyocytes, generation of restoring forces (RFs) responsible for elastic recoil involves deformation of the sarcomeric protein titin in conjunction with shortening below slack length. At the left ventricular (LV) level, recoil and filling by suction require contraction to an end-systolic volume (ESV) below equilibrium volume ( $V_{eq}$ ) as well as large-scale deformations, for example, torsion or twist. Little is known about RFs and suction in the failing ventricle. We undertook a comparison of determinants of suction in open-chest dogs previously subjected to 2 weeks of pacing tachycardia (PT) and controls. To assess the ability of the LV to contract below  $V_{eq}$ , we used a servomotor to clamp left atrial pressure and produce nonfilling diastoles, allowing measurement of fully relaxed pressure at varying volumes. We quantified twist with sonomicrometry. We also assessed transmural ratios of N2B to N2BA titin isoforms and total titin to myosin heavy chain (MHC) protein. In PT, the LV did not contract below  $V_{eq}$ , even with marked reduction of volume (end-diastolic pressure [EDP], 1 to 2 mm Hg), whereas in controls ESV was less than  $V_{eq}$  when EDP was less than  $\approx 5$  mm Hg. In PT, both systolic twist and diastolic untwisting rate were reduced, and there was exaggerated transmural variation in titin isoform and titin-to-MHC ratios, consistent with the more extensible N2BA being present in larger amounts in the subendocardium. Thus, in PT, determinants of suction at the level of the LV are markedly impaired. The altered transmural titin isoform gradient is consistent with a decrease in RFs and may contribute to these findings. (*Circ Res.* 2000;87:235-240.)

**Key Words:** suction ■ restoring forces ■ diastole ■ heart failure ■ tachycardia

Diastolic suction results from compression and/or deformation of elastic elements in the wall of the ventricle, with storage of potential energy generated during systole in the form of a restoring force (RF) that is converted to recoil and ultimately kinetic energy (mitral inflow) during filling.<sup>1-7</sup> Inherent in this definition is the requirement that the ventricle be the source of energy driving mitral flow, ie, it must actively lower its pressure below the atrium. Ventricular filling can also occur as a result of an atrioventricular pressure gradient dictated by the level of atrial pressure at the time the mitral valve opens. In this case, atrial pressure is higher than diastolic ventricular pressure whether or not suction is present.

In the cardiomyocyte, deformation of the sarcomeric protein titin during contraction below slack length is the source of a RF.<sup>8</sup> Titin is a large, filamentous protein extending from Z- to M-line of the sarcomere, with the segment spanning from near the Z-line to the A-band acting as a molecular spring. Titin is the major determinant of passive mechanical properties of the cardiomyocyte in sarcomeres stretched above and shortened below slack length.<sup>8,9</sup> In large mammals, titin exists as 2 isoforms with differing mechanical properties.<sup>9</sup> The smaller, N2B, isoform is stiffer than the larger,

N2BA, isoform. The extracellular matrix of the myocardium has also been proposed as an element that bears a RF.<sup>3</sup> With respect to ventricular mechanics, 2 mechanisms appear to contribute to suction. One is simply contraction to an end-systolic volume (ESV) below equilibrium volume ( $V_{eq}$ ), the volume at which transmural pressure in the fully relaxed state is 0.<sup>2,4-7</sup> By definition, when fully relaxed pressure is negative, a RF is present. The second mechanism is thought to reside in complex, contraction-dependent 3-dimensional deformations.<sup>3,10-17</sup> Left ventricular (LV) torsion, or twist, the counterclockwise wringing motion during systole when viewed from the base,<sup>10-17</sup> has been considered an important component of such deformations, with elastic recoil reflected in untwisting. These 2 ventricular mechanisms are closely related, because twist increases as ESV decreases.<sup>10,12,16</sup>

We previously used a servomotor that rapidly clamps left atrial pressure (LAP) during ventricular systole to lower LAP below LV diastolic pressure during the subsequent diastole, causing nonfilling diastoles during which we measured the fully relaxed LV pressure (FRP) at the ESV.<sup>7</sup> In normal, open-chest dogs, ESVs below  $V_{eq}$  were achieved under physiological filling conditions. We also found that dobutamine enhances RFs<sup>18</sup> as a result of contraction to a smaller

Received May 5, 2000; accepted June 9, 2000.

From the Cardiology Unit (S.P.B., L.N., M.D.T., M.M.L.), University of Vermont College of Medicine, Burlington, Vt, and Department of Veterinary and Comparative Anatomy, Pharmacology and Physiology (M.M., H.G.), Washington State University, Pullman, Wash.

Correspondence to Martin M. LeWinter, MD, Cardiology Unit, Fletcher Allen Health Care, 111 Colchester Ave, Burlington, VT 05401. E-mail martin.lewinter@vtmednet.org

© 2000 American Heart Association, Inc.

Circulation Research is available at <http://www.circresaha.org>

ESV and an increase in  $V_{eq}$ . On the basis of these observations, we proposed that suction is likely very important during physiological stress such as exercise. Moreover, suction should be magnified under conditions in which ESV is abnormally small, for instance, hypovolemia or cardiac tamponade.

Little is known about the ability to utilize suction in the failing ventricle. In pacing tachycardia heart failure in conscious, chronically instrumented dogs, Cheng et al<sup>19</sup> showed that, in contrast to controls, minimum LV diastolic pressure does not decrease during exercise, consistent with an impaired ability to utilize suction. Recently, Solomon et al<sup>20</sup> characterized diastolic mechanics and changes in  $V_{eq}$  in open-chest dogs with pacing failure. Nonfilling diastoles were produced by replacing the mitral valve with an electronically controlled prosthesis. Although  $V_{eq}$  was increased, contractility was so depressed in paced dogs that the LV could not contract below  $V_{eq}$  and use this mechanism of suction. In the present study, we also used the pacing model to delineate the determinants of ventricular suction. We used our servomotor to assess the relation of  $V_{eq}$  to steady-state filling conditions. We also quantified twist in relation to ESV and examined titin isoform composition.

## Materials and Methods

### Surgical Preparation and Instrumentation

Eight dogs were anesthetized with sodium thiopental, intubated, and ventilated with 100% O<sub>2</sub> and halothane. A pacing electrode was screwed into the right ventricular free wall via a limited thoracotomy. The lead was tunneled to the dorsal surface of the thorax and attached to a stimulator implanted subcutaneously. The chest was closed. Over the next 2 days the pacing rate was incrementally increased to 235 bpm and maintained at that level.

After 2 weeks, pacing rate was reduced to 150, and animals were re-anesthetized. A left thoracotomy was performed, micromanometer tip catheters were inserted in LV and left atrium (LA), a dual-conductance volume catheter was inserted in the LV, and a large-bore cannula was placed in LA.<sup>7,18,21</sup> The latter was attached to the servomotor.<sup>7,18</sup> The permanent pacemaker was disabled, and pacing electrodes were attached to the LA and connected to a stimulator.

Seven control dogs (22 to 28 kg) underwent a limited thoracotomy (without pacemaker implantation) and were instrumented and studied in the same fashion as the paced group. In 1 additional animal, instrumentation and acquisition of control data (see below) were accomplished under sterile conditions. Measurement devices were removed, and the pacemaker was implanted and activated. After 2 weeks, instrumentation and data acquisition were repeated. Dogs used for servomotor studies are referred to as the LAP clamp group.

Twist was assessed in 6 additional dogs, 3 paced and 3 nonpaced. They were prepared as above, but neither servomotor nor conductance catheter was used. Thirteen hemispheric sonomicrometer crystals (2 mm in diameter) were implanted in LV subepicardium and the right side of the interventricular septum as depicted in Figure 1. The 3 sets of crystals oriented in the plane of the minor axis were positioned at 25% (basal), 50% (equatorial), and 75% (apical) of the long axis distance. Signals were processed with a digital system in which each crystal sends a signal to and receives a signal from each of the other crystals.

### Protocol

After instrumentation, zatebradine<sup>7,18,22</sup> was administered. Then, during atrial pacing at  $\approx 90$  bpm, we manipulated steady-state LV end-diastolic pressure (EDP) from  $\approx 1$  to 2 to 9 to 10 mm Hg with transient caval and aortic constrictions.<sup>7,18</sup> In the LAP clamp group,

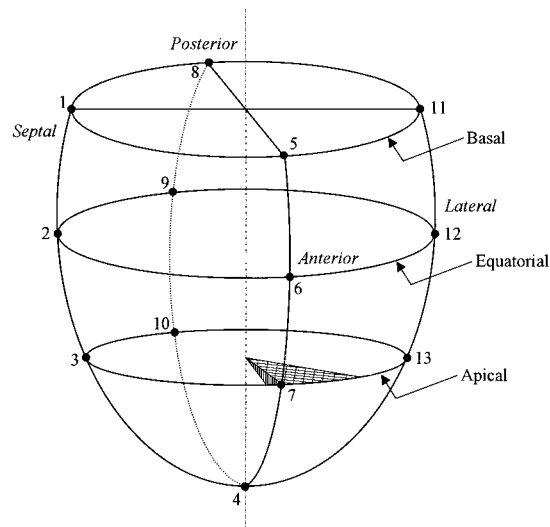


**Figure 1.** Placement of sonomicrometer crystals (see text).

FRP was measured during nonfilling diastoles at each EDP.<sup>7,18</sup> In the twist group, ultrasonic signals were recorded at each EDP.

At the end of each experiment, a full-thickness,  $\approx 1\text{-cm}^3$  specimen of LV anterior wall at the level of the equator was removed and processed as described below.

### Data Analysis

Intracardiac pressures and event timing were analyzed as previously described.<sup>7,18</sup> In LAP clamp dogs, data were grouped into EDP ranges of 1 to 2, 2 to 4, and 4 to 6 mm Hg and points selected with values closest to the midpoint of each range.

Twist was analyzed as described in the online Materials and Methods (available at <http://www.circresaha.org>). Briefly, the 3-dimensional position of each crystal was determined as a function of time and systolic twist angle  $\theta$  quantified as the angle traversed from end diastole to end systole relative to the center of each minor axis plane. Negative  $\theta$  indicates clockwise and positive  $\theta$  counter-clockwise rotation. In Figure 1, the cross-hatched area right of crystal 7 represents  $\theta$  for the apical plane. We always observed a small "overshoot" during untwisting (diagonal shaded area left of crystal 7). We also calculated peak untwisting rate in degrees per second.

The volume of the LV (including its wall) was estimated at end systole using software that applied a convex hull model to the coordinates of all 13 crystals.

### Titin Analysis

Thin layers of subendocardial, midwall, and subepicardial tissue were quick-frozen in liquid nitrogen and analyzed for titin isoforms by SDS-PAGE.<sup>23–25</sup> Tissue from mouse and human LV was also analyzed. Three titin peaks were observed in humans and dogs (2 T1 peaks at top of gel and a faint T2 peak with higher mobility) (Figure 2, lanes 2 through 5). Gaussian fits were used to separate the peaks and determine their "optical density (OD) area." The lower-mobility T1 peak is N2BA titin, containing transcripts N2A and N2B. The higher-mobility T1 peak is N2B titin, containing only N2B. The faint T2 peak is a proteolytic breakdown product.<sup>9,26</sup>

To determine the amount of titin relative to myosin heavy chain (MHC), gels were scanned and total OD of the MHC peak was determined, as well as total OD of all titin peaks. Total titin:MHC protein ratio was calculated on the basis of molecular weights.<sup>26,27</sup>

### Statistics

Data are reported as mean  $\pm$  SD. Two-way repeated-measures ANOVA was used to test for differences in EDP, FRP, titin isoforms, and titin:MHC ratios in paced and control groups. Probability values for F statistics were adjusted using the Greenhouse-Geisser method.

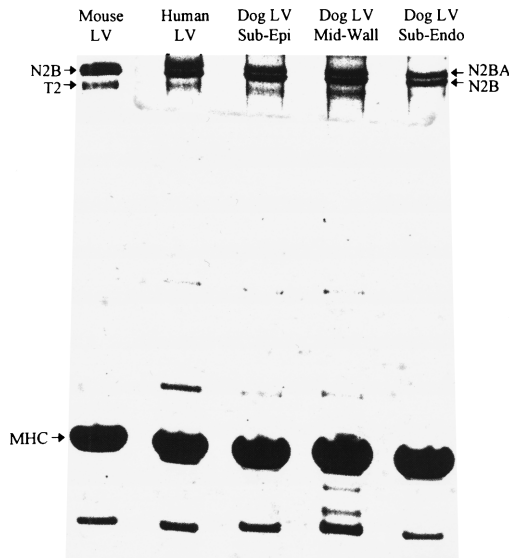


**Figure 2.** Gels showing titin peaks and MHC. Lowest-mobility band in lane 1 is N2B titin; a band with similar mobility is found in all samples. Lower-mobility band in lanes 2 to 5 is N2BA titin. Faint, higher-mobility band below N2BA and N2B titin is a proteolysis product. Sub-Epi indicates subepicardial tissue, and Sub-Endo, subendocardial tissue.

Bonferroni-corrected *t* tests were used for specific comparisons.  $P < 0.05$  was considered significant.

An expanded Materials and Methods section is available online at <http://www.circresaha.org>.

## Results

Just after zatebradine administration and initiation of atrial pacing, heart rate was  $89 \pm 1$  and  $91 \pm 4$  bpm, EDP was  $3.9 \pm 2.5$  and  $8.1 \pm 2.7$  mm Hg ( $P < 0.05$ ), and peak LV systolic pressure was  $96 \pm 8$  and  $108 \pm 7$  mm Hg in the control and paced LAP clamp groups, respectively.

Figure 3 displays the relation between EDP and FRP for LAP clamp groups during nonfilling diastoles at each EDP range. Controls developed a negative FRP at EDP below  $\approx 5$  mm Hg, indicating the presence of a RF. In contrast, even at EDP 1 to 2 mm Hg, paced dogs had a FRP  $> 0$  mm Hg. The

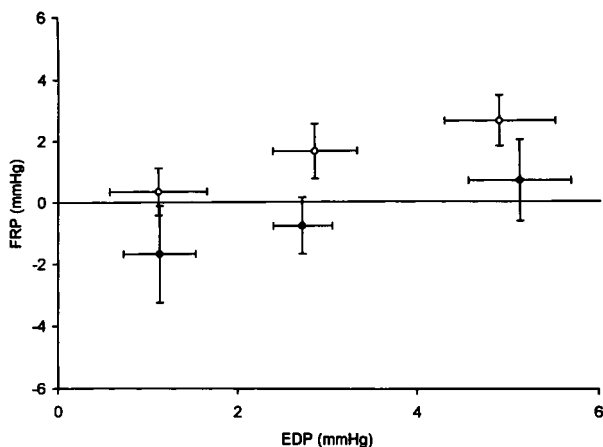


**Figure 3.** Relationship between EDP and FRP at selected EDP ranges for paced and control dogs (see text).

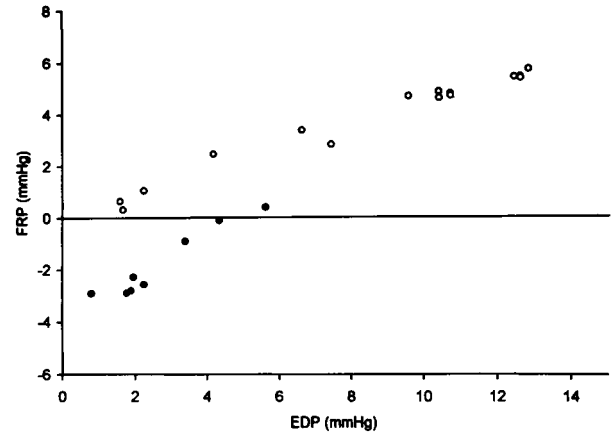
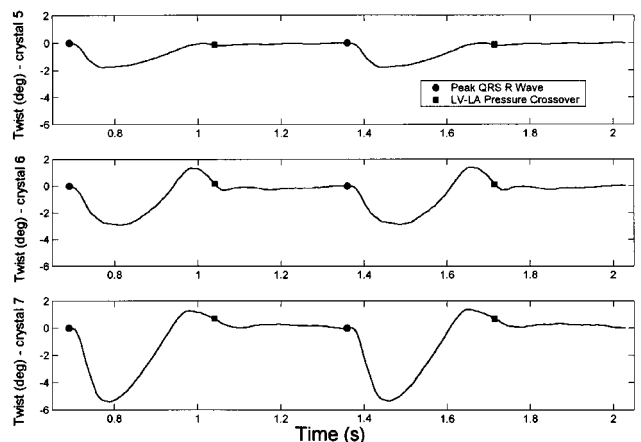


**Figure 4.** Relationship between EDP and FRP in dog with measurements before and after pacing.

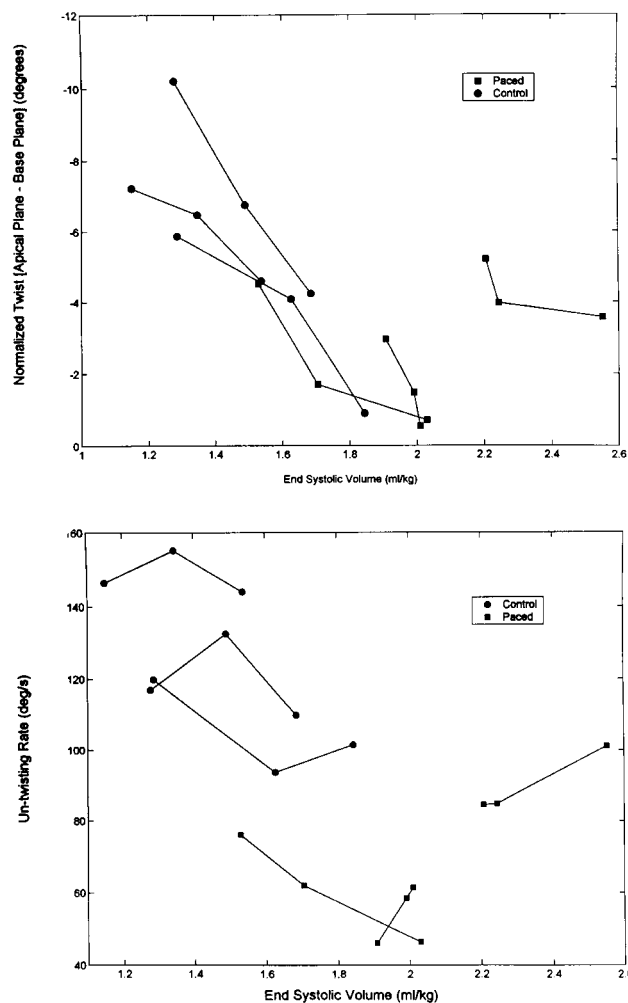
difference in FRP between controls and paced dogs was significant ( $P < 0.05$ ) at each EDP range.

Figure 4 displays data from the dog in whom serial measurements were made before and after pacing. After pacing, FRP remained positive, even at very low EDPs.

Figure 5 shows an example of  $\theta$  versus time for basal, equatorial, and apical planes in a paced dog, as well as timing markers for end diastole (peak QRS R wave) and mitral valve opening (LV-LA pressure crossover). As expected,<sup>10,12,13,15</sup> twist increased from base to apex. This pattern was present in all dogs regardless of hemodynamic conditions. Note also the overshoot during untwisting. As reported previously,<sup>10–17</sup> untwisting was largely complete by the time of mitral valve opening. Figure 6 (top) shows apical  $\theta$  in the 3 paced and 3 control dogs as a function of ESV. For each dog, values are shown at ESVs corresponding to EDPs at the high and low end of the EDP range from 1 to 2 to 9 to 10 mm Hg and an EDP in the middle of this range. As expected, in each dog, twist increased as ESV decreased. Two of the paced dogs appeared to fall on a roughly similar relationship between twist and ESV as the control dogs.  $\theta$  was smaller in these dogs, because their ESVs tended to be larger. The third paced dog had the largest ESVs, yet had  $\theta$  values somewhat larger



**Figure 5.** Twist angle  $\theta$  vs time for basal, midventricular, and apical planes (top to bottom) in a representative paced dog (see text).



**Figure 6.** Top, apical twist angle  $\theta$  as function of ESV in control and paced dogs. Bottom, peak apical untwisting rate as function of ESV in control and paced dogs.

than the other paced dogs. Nonetheless, the highest twist value in this dog was considerably smaller than the values recorded at the lower ESVs in the control dogs. Thus, at lower EDPs, this dog also had smaller twist values than control dogs. Figure 6 (bottom) shows peak untwisting rate for the same data points. In contrast to  $\theta$ , there was no consistent change in untwisting rate as ESV decreased. However, untwisting rate was systematically larger in the control dogs, even at overlapping ESV ranges. Similar to  $\theta$ , the paced dog with the largest ESVs had somewhat larger untwisting rates than the 2 other paced dogs.

Figure 7 displays transmural N2BA:N2B titin isoform ratios. There were roughly equal proportions of both isoforms. However, as reported in normal pigs,<sup>9</sup> in controls the ratio decreased progressively from subendocardium ( $1.03 \pm 0.35$ ) to subepicardium ( $0.83 \pm 0.26$ ). The difference between subendocardium and subepicardium was significant ( $P < 0.05$ ). In paced dogs, the same transmural pattern was observed ( $P < 0.05$ ), but the ratio was larger in the subendocardium ( $1.29 \pm 0.27$ ) and smaller in the subepicardium ( $0.67 \pm 0.23$ ). As a result, the subendocardial-subepicardial gradient in isoform ratio was much larger in paced dogs.

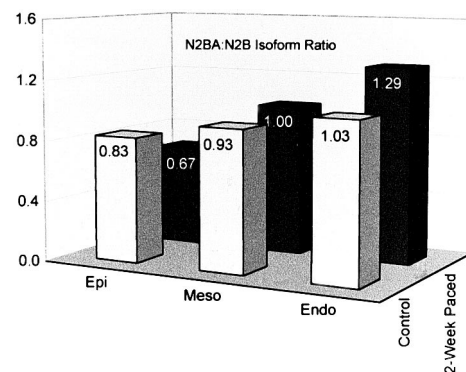


**Figure 7.** Transmural ratios of N2BA to N2B titin in control and paced dogs. Epi indicates subepicardial; meso, midwall; and endo, subendocardial.

However, the difference in gradient between paced and control dogs did not reach statistical significance ( $P = 0.099$ ). To further explore the difference in isoform expression between paced and control animals, we measured transmural ratios of total titin:MHC protein. If the larger transmural gradient in isoform ratio seen in paced animals is real, the total titin:MHC ratio should demonstrate a change in transmural gradient (because of the larger molecular weight of N2BA titin). As expected on the basis of isoform ratios, in control dogs the titin:MHC ratio increased from subepicardium ( $0.22 \pm 0.02$ ) to subendocardium ( $0.27 \pm 0.02$ ,  $P < 0.05$ ). Also consistent with the isoform ratio results, the subepicardial titin:MHC ratio was smaller in paced dogs ( $0.17 \pm 0.05$ ), and the subepicardial ratio was larger ( $0.29 \pm 0.03$ ). Furthermore, the transmural subepicardial-subendocardial titin:MHC ratio gradient was significantly larger in paced compared with control dogs ( $P < 0.03$ ).

## Discussion

The ability of the LV to generate RFs during contraction and utilize suction as a mechanism of filling during diastole depends in part on whether and how far the ESV is below  $V_{eq}$ .<sup>1-7</sup> Even without an external load, the LV wall contains residual strains,<sup>28</sup> but these presumably do not contribute to suction. Three-dimensional deformations occurring during contraction are believed to serve as additional mechanisms of RF generation.<sup>10-17</sup> Twist is one manifestation of such deformations. Deformation of the extracellular matrix has also been proposed as the source of a RF.<sup>3</sup> Last, because titin isoforms have differing mechanical properties,<sup>9</sup> their expression ratio and regional distribution could influence RFs.

In the present study, we found that after only 2 weeks of pacing tachycardia, the LV was incapable of contracting to an ESV below  $V_{eq}$ , even at EDPs as low as 1 to 2 mm Hg. Although a RF might have been present at even lower EDPs, this effectively eliminates contraction below  $V_{eq}$  as a mechanism of suction. In the twist group, over the range of EDPs studied, ESV was larger in paced dogs than in controls. Thus, it is likely that increased ESV due to contractile dysfunction is a major factor accounting for impaired suction. Because the LV did not actually reach  $V_{eq}$  during the caval constriction protocol, in the paced dogs we cannot specify whether  $V_{eq}$  was altered. Recently, Solomon et al<sup>20</sup> studied diastolic mechanics in dogs



subjected to 4 weeks of rapid pacing and reported a substantial increase in  $V_{eq}$ , which was ascribed to remodeling.<sup>29</sup> They also concluded that depressed contractility prevented the LV from achieving ESVs below  $V_{eq}$ , despite the increase in  $V_{eq}$ . A significant difference between our study and that of Solomon et al<sup>20</sup> is that nonfilling diastoles were produced by excising the mitral valve during cardiopulmonary bypass and replacing it with an electronically controlled prosthesis fixed in a closed position during diastole. Cardiopulmonary bypass and excision of the mitral valve with disruption of its apparatus depress contractile function and alter LV volume and shape.<sup>30–33</sup> Accordingly, our methods likely result in a somewhat more physiological preparation. Solomon et al<sup>20</sup> also did not relate FRP to steady-state LVEDP and did not examine twist or titin isoforms.

We found that twist was reduced in paced dogs. Although the numbers of experiments were small, the decrease appeared to be mainly due to the fact that ESVs tended to be larger in these animals. Untwisting rate was also reduced in the paced dogs; in this case the reduction appeared to be independent of changes in ESV. Because untwisting presumably reflects elastic recoil, this observation suggests a change in the behavior of the “springs” responsible for recoil such that for a given amount of deformation the rate of return to the resting state is slower in the failing ventricle. Changes in twist and untwisting may constitute a second mechanism of impaired suction. However, we also confirmed that untwisting was largely complete by the time of mitral valve opening. Thus, twist-untwisting may actually make a minor contribution to filling or perhaps the relatively small amount of untwisting occurring after mitral valve opening is sufficient to cause suction. Alternatively, the twist-associated RF might be converted to some other deformation in the wall that facilitates suction after mitral valve opening.

Although the magnitude of twist is inversely related to ESV, contraction-dependent deformations that contribute to suction may be considered as distinct from a RF generated solely by contraction below  $V_{eq}$ . During the course of a nonfilling diastole, these deformations return to the resting state as the ventricle relaxes, ie, they do not influence the FRP. Thus, suction can be envisioned as being caused by both a RF related to systolic deformations and a RF that is still present after completion of relaxation at ESV below  $V_{eq}$ . It is even possible that at the time the mitral valve opens, before relaxation is complete, a contraction-dependent RF is present that causes suction even though fully relaxed pressure is  $\geq 0$ .

We documented a transmural gradient in titin isoforms in control dogs, with more N2BA in subendocardium and more N2B in subepicardium. The springlike region of titin extends from near the Z-line to its attachment to the thick filament and is composed of 2 main segment types, the so-called PEVK segment and serially linked immunoglobulin-like domains flanking the PEVK segment.<sup>8,9</sup> N2B titin contains a unique 572-amino acid sequence that is also extensible. N2BA titin has a longer extensible region and therefore develops less force when stretched. The presence of N2BA titin explains the lower passive stiffness of pig compared with mouse cardiomyocytes, because the latter express only N2B titin.<sup>9</sup> The larger proportion of the more extensible N2BA isoform in subendocardium may

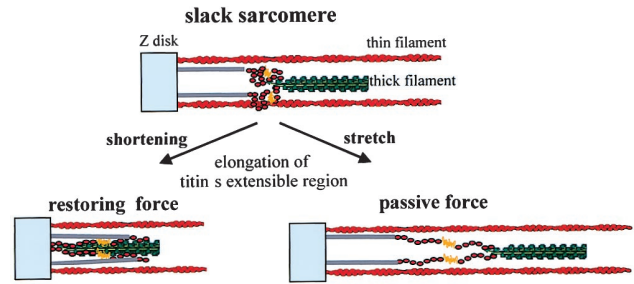


**Figure 8.** Schematic of behavior of titin during extension above slack length and shortening below slack length (see text).

have functional significance in that most thickening and thinning takes place in the inner half of the wall.

We found that the transmural titin isoform ratio gradient was exaggerated in paced dogs. Although this did not achieve statistical significance, the significant difference in total titin:MHC gradient strongly supports a true change in isoform ratios. (Because there is a fixed stoichiometry between titin and MHC, their ratio may be more reliable than the isoform ratio for delineating isoform variations, because it does not require curve fitting to separate electrophoretic peaks.) It is unknown whether or how the 2 isoforms influence slack length or passive mechanical behavior below slack length. Moreover, our studies do not prove a cause-and-effect relationship between titin changes and reduced RFs. However, it is reasonable to assume that just as the N2BA isoform causes a less steep relation between tension and sarcomere length during stretch above slack length, it also causes a less steep relation below slack length, with the resulting RF being smaller in magnitude. This is consistent with the mechanism of RF development by titin proposed by Helmes et al<sup>8</sup> (Figure 8). This mechanism is based on the finding that the titin segment just adjacent to the Z-line is inextensible and incompressible (because of its actin-binding property) and that when sarcomeres contract below slack length, thick filaments move into this incompressible region. This results in stretch of the extensible segment in a direction opposite that during lengthening above slack length and production of a force that returns the shortened sarcomere toward slack length.<sup>8</sup> Thus, the larger proportion of the more extensible N2BA isoform in the inner portion of the wall in paced animals could contribute to reduced RF generation, once again because most thickening and thinning occur in this portion of the wall. Although the proportional change in subendocardial N2BA isoform was only  $\approx 25\%$ , the difference in stiffness between the 2 isoforms is quite marked. The idea that individual cardiomyocytes from hearts subjected to rapid pacing differ with respect to RF generation is supported by Zile et al,<sup>34</sup> who found that unloaded cardiomyocytes obtained from paced dogs have a reduced ratio of lengthening rate to fractional shortening.

It is also tempting to speculate that the substantial change in transmural isoform gradient is related to changes in large-scale deformations such as twist-untwisting. With respect to RFs, these large-scale deformations presumably reflect the behavior of functional springs extending between different fiber bundles in the wall. An alteration in isoform distribution across the wall might interfere with the behavior of these springs.

The extracellular matrix has also been proposed as an element that can bear a RF.<sup>3</sup> Thus, remodeling related to dissolution of the matrix observed in pacing tachycardia<sup>29</sup> could also contribute to impaired RFs. Against this, however, is the observation that collagen makes a very small contribution to stiffness near slack length.<sup>23</sup>

In control dogs, FRP did not become negative until EDP reached  $\approx 5$  mm Hg, a slightly lower value than we reported previously in normal, open-chest dogs.<sup>7</sup> Because our data analyses require quantification of small pressure differences, unavoidable measurement variation may have contributed to this difference. Additionally, in our previous study,<sup>7</sup> anesthesia was accomplished with pentobarbital, whereas halothane was used in this study. In our preparation, Veq occurs at a LVEDP at the lower end of the physiological range. It might therefore be argued that RFs generated as a result of contraction below Veq are unimportant under normal physiological conditions and that loss of the ability to generate a RF by this mechanism has little functional consequence. However, open-chest, anesthetized conditions inevitably depress contractility and probably impair the ability of the LV to generate RFs. Moreover, RFs are expected to be largest when contractility is high and ESV is small, for example, during exercise. Our previous results demonstrating that dobutamine increases Veq<sup>18</sup> suggest that adrenergic stimulation facilitates RF generation. Thus, there is a strong likelihood that under physiological conditions RFs and suction are more important than suggested by our data. Finally, because successful therapy of heart failure usually results in decreased ESV, it is possible that in the failing heart the effects of impaired suction are most evident when patients are compensated.

### Acknowledgments

This research was supported by NIH Grants HL51201 and HL61497.

### References

- Brecher GA. Critical review of recent work on ventricular diastolic suction. *Circ Res*. 1968;6:554–566.
- Hori M, Yellin EL, Sonnenblick EH. Left ventricular diastolic suction as a mechanism of ventricular filling. *Jpn Circ J*. 1982;46:124–129.
- Robinson TF, Factor SM, Sonnenblick EH. The heart as a suction pump. *Sci Am*. 1986;254:84–91.
- Ingels NB Jr, Daughters GT II, Nikolic SD, DeAnda A, Moon MR, Bolger AF, Komeda M, Derby GC, Yellin EL, Miller DC. Left atrial pressure-clamp servomechanism demonstrates LV suction in canine hearts with normal mitral valves. *Am J Physiol*. 1994;267:H354–H362.
- Yellin EL, Hori M, Yoran C, Sonnenblick EH, Gabby S, Frater RWM. Left ventricular relaxation in the filling and nonfilling intact canine heart. *Am J Physiol*. 1986;250:H620–H629.
- Nikolic S, Yellin EL, Tamura K, Vetter H, Tamura T, Meisner JS, Frater RWM. Passive properties of the canine left ventricle: diastolic stiffness and restoring forces. *Circ Res*. 1988;62:1210–1222.
- Bell SP, Fabian J, Higashiyama A, Chen Z, Tischler MD, Watkins MW, LeWinter MM. Restoring forces assessed with left atrial pressure clamps. *Am J Physiol*. 1996;270:H1015–H1020.
- Helmes M, Trombitas K, Granzier H. Titin develops restoring force in rat cardiac myocytes. *Circ Res*. 1996;79:619–626.
- Cazorla O, Freiburg A, Helmes M, Centner T, McNabb M, Wu Y, Trombitas K, Labeit S, Granzier H. Differential expression of cardiac titin isoforms and modulation of cellular stiffness. *Circ Res*. 2000;86:59–67.
- Hansen DE, Daughters GT II, Alderman EL, Ingels NB Jr, Miller DC. Torsional deformation of the left ventricular midwall in human hearts with intramyocardial markers: regional heterogeneity and sensitivity to the inotropic effects of abrupt rate changes. *Circ Res*. 1988;62:941–952.
- Beyar R, Yin FCP, Hausknecht M, Weisfeldt ML, Kass DA. Dependence of left ventricular twist-radial shortening relations on cardiac cycle phase. *Am J Physiol*. 1989;257:H1119–H1126.
- Ingels NB Jr, Hansen DE, Daughters GT II, Stinson EB, Alderman EL, Miller DC. Relation between longitudinal, circumferential, and oblique shortening and torsional deformation in the left ventricle of the transplanted human heart. *Circ Res*. 1989;64:915–927.
- Buchalter MB, Weiss JL, Rogers WJ, Zerhouni EA, Weisfeldt ML, Beyar R, Shapiro EP. Noninvasive quantification of left ventricular rotational deformation in normal humans using magnetic resonance myocardial tagging. *Circulation*. 1990;81:1236–1244.
- Rademakers FE, Buchalter MB, Rogers WJ, Zerhouni EA, Weisfeldt ML, Weiss JL, Shapiro EP. Dissociation between left ventricular untwisting and filling. *Circulation*. 1992;85:1572–1581.
- Gibbons Kroeker CA, Terkeurs HEDJ, Knudtson ML, Tyberg JA, Beyar R. An optical device to measure the dynamics of apex-rotation of the left ventricle. *Am J Physiol*. 1993;265:H1444–H1449.
- Gibbons Kroeker CA, Tyberg JV, Beyar R. Effects of load manipulations, heart rate, and contractility on left ventricular apical rotation. *Circulation*. 1995;92:130–141.
- DeAnda A Jr, Komeda M, Nikolic SD, Daughters GT 2nd, Ingels NB, Miller C. Left ventricular function, twist, and recoil after mitral valve replacement. *Circulation*. 1995;92(suppl II):II-458–II-466.
- Bell SP, Fabian J, LeWinter MM. Effects of dobutamine on left ventricular restoring forces. *Am J Physiol*. 1998;275:H190–H194.
- Cheng CP, Noda T, Nozawa T, Little WC. Effect of heart failure on the mechanism of exercise-induced augmentation of mitral valve flow. *Circ Res*. 1993;72:795–806.
- Solomon SB, Nikolic SD, Glantz SA, Yellin EL. Left ventricular diastolic function of remodeled myocardium in dogs with pacing-induced heart failure. *Am J Physiol*. 1998;274:H945–H954.
- Steendijk P, Van der Velde ET, Baan J. Left ventricular stroke volume by single and dual excitation of conductance catheter in dogs. *Am J Physiol*. 1993;264:H2198–H2207.
- Chen Z, Slinker BK. The sinus node inhibitor UL-FS49 lacks significant inotropic effect. *J Cardiovasc Pharmacol*. 1991;19:264–271.
- Granzier HL, Irving TC. Passive tension in cardiac muscle: contribution of collagen, titin, microtubules, and intermediate filaments. *Biophys J*. 1995;68:1027–1044.
- Granzier HL, Wang K. Gel electrophoresis of giant proteins: solubilization and silver-staining of titin and nebulin from single muscle fiber segments. *Electrophoresis*. 1993;14:56–64.
- Neuhoff V, Arold N, Taube D, Ehrhardt W. Improved staining of proteins in polyacrylamide gels including isoelectric focusing gels with clear background at nanogram sensitivity using Coomassie brilliant blue G-250 and R-250. *Electrophoresis*. 1988;9:255–261.
- Granzier H, Helmes M, Trombitas K. Nonuniform elasticity of titin in cardiac myocytes: a study using immunoelectron microscopy and cellular mechanics. *Biophys J*. 1996;70:430–442.
- Labeit S, Kolmerer B. Titins: giant proteins in charge of muscle ultrastructure and elasticity. *Science*. 1995;270:293–296.
- Omens JH, Fung YC. Residual strains in the rat left ventricle. *Circ Res*. 1990;66:37–45.
- Spinale FG, Tomita M, Zellner JL, Cook JC, Crawford FA, Zile MR. Collagen remodeling and changes in LV function during development and recovery from supraventricular tachycardia. *Am J Physiol*. 1991;261:H308–H318.
- David TE, Uden DE, Strauss HD. The importance of the mitral valve apparatus in left ventricular function after correction of mitral regurgitation. *Circulation*. 1983;68(suppl II):II-76–II-82.
- Hansen D, Cahill P, DeCampi W, Harrison D, Derby G, Mitchell R, Mill DG. Valvular-ventricular interaction: importance of the mitral apparatus in canine left ventricular systolic performance. *Circulation*. 1986;73:1310–1320.
- Hansen DE, Sarris GE, Niczyporuk MA, Derby GC, Cahill PD, Miller DC. Physiologic role of the mitral apparatus in left ventricular regional mechanics, contraction synergy, and global systolic performance. *J Thorac Cardiovasc Surg*. 1989;97:521–533.
- Rozich J, Carabello B, Usher B, Kratz J, Bell A, Zile M. Mitral valve replacement with and without chordal preservation in patients with chronic mitral regurgitation. *Circulation*. 1992;86:1718–1726.
- Zile MR, Mukherjee R, Clayton C, Kato S, Spinale FG. Effects of chronic supraventricular pacing tachycardia on relaxation rate in isolated cardiac muscle cells. *Am J Physiol*. 1995;268:H2104–H2113.